

DTIC FILE COPYUni
SEC**AD-A223 996**Form Approved
OMB No 0704-0188

REPORT DOCUMENTATION PAGE

1a REPORT SECURITY CLASSIFICATION Unclassified		1b RESTRICTIVE MARKINGS	
2a SECURITY CLASSIFICATION / DOWNGRADING SCHEDULE SELECTED SUN 29 1990		3 DISTRIBUTION/AVAILABILITY OF REPORT Approved for public release; Distribution unlimited	
4 PERFORMING ORGANIZATION REPORT NUMBER(S) GL-TR-90-0151		5 MONITORING ORGANIZATION REPORT NUMBER(S)	
6a NAME OF PERFORMING ORGANIZATION Geophysics Laboratory	6b OFFICE SYMBOL (If applicable) PHS	7a NAME OF MONITORING ORGANIZATION	
6c ADDRESS (City, State, and ZIP Code) Hanscom AFB Massachusetts 01731-5000		7b ADDRESS (City, State, and ZIP Code)	
8a NAME OF FUNDING/SPONSORING ORGANIZATION	8b OFFICE SYMBOL (If applicable)	9 PROCUREMENT INSTRUMENT IDENTIFICATION NUMBER	
8c ADDRESS (City, State, and ZIP Code)		10 SOURCE OF FUNDING NUMBERS	
		PROGRAM ELEMENT NO 61102F	PROJECT NO 2311
		TASK NO G3	WORK UNIT ACCESSION NO 26
11 TITLE (Include Security Classification) Line Asymmetries and Vertical Velocities Observed with a Narrow-band Filter			
12 PERSONAL AUTHOR(S) Stephen L. Keil, Domenico Bonaccini*, Peter Tamblyn**, Larry November**			
13a TYPE OF REPORT Reprint	13b TIME COVERED FROM _____ TO _____	14 DATE OF REPORT (Year, Month, Day) 1990 June 20	15. PAGE COUNT 14
16 SUPPLEMENTARY NOTATION* Instituto di Astronomia, Firenze, Italy **National Solar Observatory Sacramento Peak, Sunspot NM 88349 - Reprinted from High Spatial Resolution Solar Observations, ed. O. von der Luhe, National Solar Observatory, Sunspot NM Aug 1989 pp 277-285			
17. COSATI CODES		18 SUBJECT TERMS (Continue on reverse if necessary and identify by block number) Solar absorption lines, Solar velocity fields, Birefringent filters	
19. ABSTRACT (Continue on reverse if necessary and identify by block number)			
<p>A Fabry-Perot filter was combined with the Sacramento Peak Universal Birefringent Filter (UBF) to obtain a filter system with a 20 milli-angstrom band pass. Filtergrams were obtained at disk center in the Ca I line at 6162 angstroms under excellent seeing conditions. We have used this data to measure line profiles of resolved granular features and to make maps of the vertical flow associated with the granulation. In this paper we present ensemble average profiles for bright granular features, dark lanes, up-flows and down-flows. The results shown here represent only a very preliminary look at the data set. A time sequence of these filtergrams is currently being processed and will allow much better separation of effects due to oscillations from those due to the granulation.</p>			
20 DISTRIBUTION/AVAILABILITY OF ABSTRACT <input type="checkbox"/> UNCLASSIFIED/UNLIMITED <input checked="" type="checkbox"/> SAME AS RPT. <input type="checkbox"/> DTIC USERS		21. ABSTRACT SECURITY CLASSIFICATION Unclassified	
22a NAME OF RESPONSIBLE INDIVIDUAL Claire Caulfield		22b TELEPHONE (Include Area Code) (617) 377-4555	22c OFFICE SYMBOL GL/SULLP

HIGH SPATIAL RESOLUTION SOLAR OBSERVATIONS

Proceedings of the Tenth Sacramento Peak
Summer Workshop, Sunspot, New Mexico

22 - 26 August 1988



National Solar Observatory / Sacramento Peak
Sunspot, New Mexico 88349, USA

BEST
AVAILABLE COPY

Line asymmetries and vertical velocities observed with a narrow-band filter

Stephen L. Keil

Air Force Geophysics Laboratory, Sacramento Peak Observatory,
Sunspot, NM 88349, USA

Domenico Bonaccini

Istituto di Astronomia, Firenze, Italy

Peter Tamblyn and Larry November

National Solar Observatory, Sacramento Peak, Sunspot, NM 88349, USA

Abstract

A Fabry-Perot filter was combined with the Sacramento Peak Universal Birefringent Filter (UBF) to obtain a filter system with a 20 milli-angstrom band pass. Filtergrams were obtained at disk center in the Ca I line at 6162 angstroms under excellent seeing conditions. We have used this data to measure line profiles of resolved granular features and to make maps of the vertical flow associated with the granulation. In this paper we present ensemble average profiles for bright granular features, dark lanes, up-flows and down-flows. The results shown here represent only a very preliminary look at the data set. A time sequence of these filtergrams is currently being processed and will allow much better separation of effects due to oscillations from those due to the granulation.

*Reprints: narrowband filters; bandpass filters;
birefringent filters. 1974*

1. Introduction

The problem of measuring the properties of flows and structures in the solar atmosphere is a question of obtaining good spatial and spectral resolution simultaneously. Spatial resolution is needed to resolve the features while spectral resolution is needed to obtain diagnostics of velocities, temperatures, and other properties of the gas. Spectrographs provide good spectral resolution, but generally give spatial resolution in only one dimension, or trade spatial for temporal resolution in two dimensions. Filter systems generally provide good spatial coverage and resolution, but sacrifice spectral resolution. The development of a very narrow band filter system has given us the ability to do spectroscopy at very high spatial resolution, with acceptable temporal resolution for studying many solar phenomena. However, the discrete temporal sampling of the line does give a changing seeing condition with wavelength. This problem is addressed in the data reduction method.

In this paper, we apply this new instrumentation to the problem of measuring flows in the solar photosphere and temperature minimum region as a function of height in the solar atmosphere. The data is from a preliminary run with the instrument and work is in progress on using time sequences to separate out the various velocity fields in the atmosphere.

2. Observations and Reduction

The observations were obtained using a narrow band filter system with a 20 milli-angstrom band pass (Bonaccini and Smartt, 1988). The Ca I line at 6162 angstroms was scanned in 10 milli-angstrom steps, starting in the blue-wing and stepping towards the red. A total of 71 spectral points were obtained as well as three points in the true continuum to the red of the line. The filtergram at each wavelength consists of 128x128 spatial points, with 0.3" sampling. The observations were made at disk center. A mean line profile was obtained by averaging all of the spatial points on each filtergram. A correction factor for each filtergram was found by adjusting the mean profile to match the 6162 profile from the Jungfraujoch Atlas. The wavelength reference was established by calibrating the filter at sun center, on the Fe I 5576.099 angstrom line. The tuning formulas for the filter have been previously determined (Bonaccini and Stauffer, 1988).

Because it takes a minute or so to scan completely through the line, seeing changes occur during the observation. This introduces image motion and image stretch (local displacements of the image). To remove these distortions and motions, the destretching algorithm of November (1986) was applied to the data. In this method, a displacement vector map is found by maximizing the local cross correlation between the data and a reference frame. These displacements are then applied to the data image using quadratic interpolation. The process was complicated because the actual structure on the images changes as we scan in wavelength. This problem was handled by using a temporal, and limited spectral average of the data to define a set of reference images, and then destretching the individual images with respect to these reference images.

The corrected intensity images are then used to obtain a line profile at each spatial point on the sun. We have used these profiles to generate velocity maps, vertical velocity slices and to generate ensemble average line profiles for various bins that depend on either continuum intensity or on velocity deep in the atmosphere.

3. Results

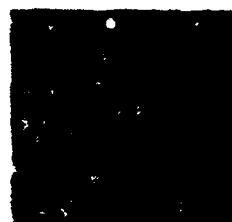
3.1 Intensities and Velocities Through the Line

Figure 1a shows the intensity images at several positions in the spectral line from the blue to the red wing. Figure 1b shows similar velocity maps (line bisector position maps) observed at various points in the line. All intensities are placed on the same scale as the Jungfraujoch Atlas, thus dark means darker than the atlas profile and bright means brighter than the atlas profile at a given wavelength. Bisectors were found at equally spaced intensities based on this same scale, thus, at a given intensity we may or may not find a bisector, depending upon the strength of the line at the point on the sun. The velocity maps have had a local spatial average, generated from a velocity map near the line core, removed to suppress the effects of the 5 minute oscillations. Although this does not completely suppress the oscillations, it helps make the granular flows easier to see (Keil, 1980).

These maps reveal a number of interesting features. The amplitude of the velocity fluctuations decreases as we go from the line wings into the line core (i.e. with height). The spatial size of velocity and intensity features increases with height (depth in the line) with only a few of the granules still visible near line core. The correlation between the velocities seen in the line wings and the continuum intensity is about 0.6, which is somewhat lower than normally observed value of 0.8-0.9 (Canfield and Mehlretter, 1973). This may result from the time delay in scanning the two sides of the spectral line for each velocity determination which permits a number of features to evolve so that the bisector maps in the wings represent a composite of features. The strongest down-flows tended to be concentrated in a few large dark features, while the dark lanes showed a down-flow of $200-400 \text{ ms}^{-1}$ (unrestored for instrumental and atmospheric smearing).

Ca I 6162 - Intensity Scans

6161.86



6161.97



6162.05



6162.15



6162.18



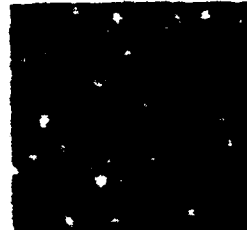
6162.21



6162.31



6162.39



6162.50



— 30" —

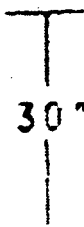


Figure 1a. Filtergrams at several selected wavelengths starting in the blue-wing of the Ca I 6162 Å line (upper-left) and scanning to the red-wing (lower-right). Line core is at 6162.18 Å. Each frame covers an area approximately 30" x 30".

Accession For	
NTIS GRA&I	<input checked="" type="checkbox"/>
DTIC TAB	<input type="checkbox"/>
Unannounced	<input type="checkbox"/>
Justification	
By _____	
Distribution/ _____	
Availability Codes	
Dist	Avail and/or Special
A-120	



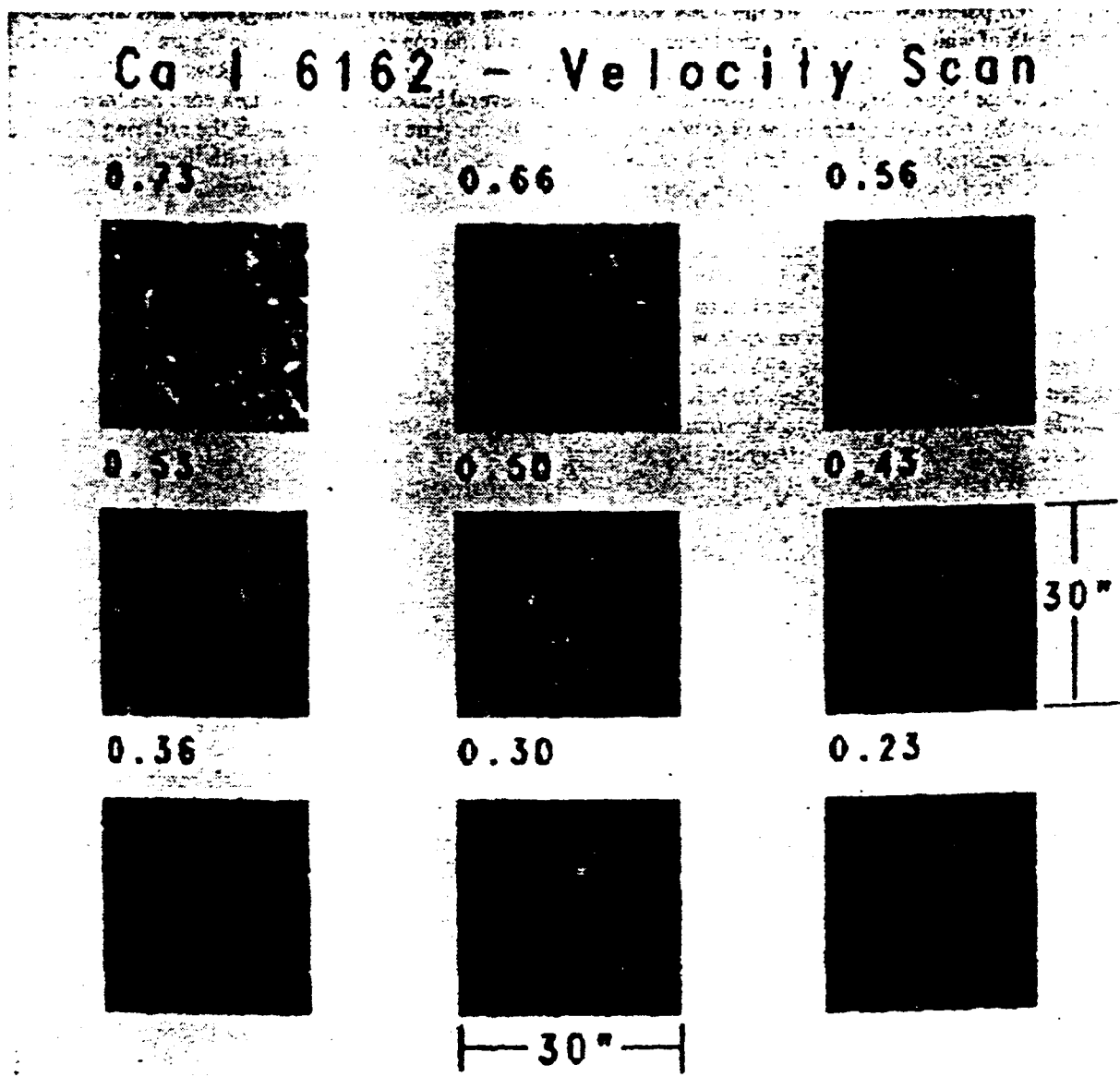


Figure 1b. Dopplergrams at several selected bisector levels are shown. The bisector level is shown above each Dopplergram starting from a level of 73% of the continuum intensity of the Jungfraujoch Atlas profile (upper-left) and ending at a level of 23% (lower-right). Each frame covers an area approximately $30'' \times 30''$. The images are plotted on a scale from $+2.5 \text{ km s}^{-1}$ (bright) to -2.5 km s^{-1} (dark) where down-flows (redshifts) are positive and up-flows (blueshifts) are negative. Thus granular up-flows appear as dark features and intergranular spaces as bright lanes.

Of particular interest are the flows associated with an apparently exploding granule and large dark pore, both of which can be seen in the lower center portion of the continuum frames in Figure 1a. Figure 2a is a blow-up of the intensity maps in a region surrounding the exploding granule at various wavelengths through the line while Figure 2b shows the associated velocities at several bisector levels. A dark core has formed in the center of the granule as seen in the blue wing of the line. By the time the scan reaches the red wing (50sec) the surrounding bright regions appear to have expanded. A strong up-flow is associated with the entire granule, including the dark core. Apparently, the core of the granule has cooled before the associated flow has decreased.

Figures 3a and b are identical to Figures 2a and b, except a region surrounding the dark pore is shown. The pore is seen to have a strong up-flow in its center, surrounded by strong down-flows. The pore appears to elongate in the core of the line with a small bright feature appearing in the lower left side of the pore. The velocity field maintains its shape with height (depth in the line), with a decreasing amplitude. The velocity profile of the pore could explain why some authors report up-flows and others down-flows in this type of feature. Placement of the spectrograph slit can effect the resultant measurement.

3.2 Vertical Slices

Figure 4 shows an image of the continuum intensity (above), along with maps of intensity and velocity for a vertical cross section through the data. The cross section was taken along a horizontal line shown on the figure. The intensities are from 30 wavelength steps to the blueward side of the line core. The vertical velocities were generated by measuring the bisector point at 33 equally spaced intensity levels through the line. The five minute oscillations have been suppressed by removing a local mean velocity which was obtained by averaging over regions of $10'' \times 10''$ on the line center images. The vertical axis of the slices represents equally spaced bisector levels, not true heights in the atmosphere. The bottom edge of the velocity slice is ragged because we measure each of the line profiles relative to the mean profile, and we take our intensity steps with respect to the mean profile. Part of the profiles are brighter and part darker than the mean. Up-flows are shown as dark (negative velocities) and down-flows as bright in the figure. Some of the up-flows appear to spread with height.

3.3 Average Line Profiles

In spatially unresolved measurements of photospheric line bisectors, the correlation between velocity and temperature fluctuations associated with fine-scale solar granulation produces the well known convective blue-shift and distinctive C-shape of the bisectors (see for example the review by Dravins, 1982). Unfortunately, using the observed, spatially unresolved bisectors to deduce properties of the granulation does not lead to unique models. Temperature distributions, velocity gradients and correlation between velocity and temperature all influence the shapes. High spatial resolution measurements of line profiles can help distinguish between the various possible models.

Spatially resolved line bisector shapes can be used as tracers of the gradient of the vertical flow in the atmosphere. Steep velocity gradients should produce highly asymmetric bisectors. The relationship between bisector shape and velocity gradient is complicated by other factors such as the temperature distribution, velocity temperature correlations and spatial resolution of the observations. In order to reveal any trends between the flows and the bisector shapes, we have averaged profiles together based on either the observed flow or observed brightness deep in the atmosphere, i.e. where the granulation pattern is most obvious.

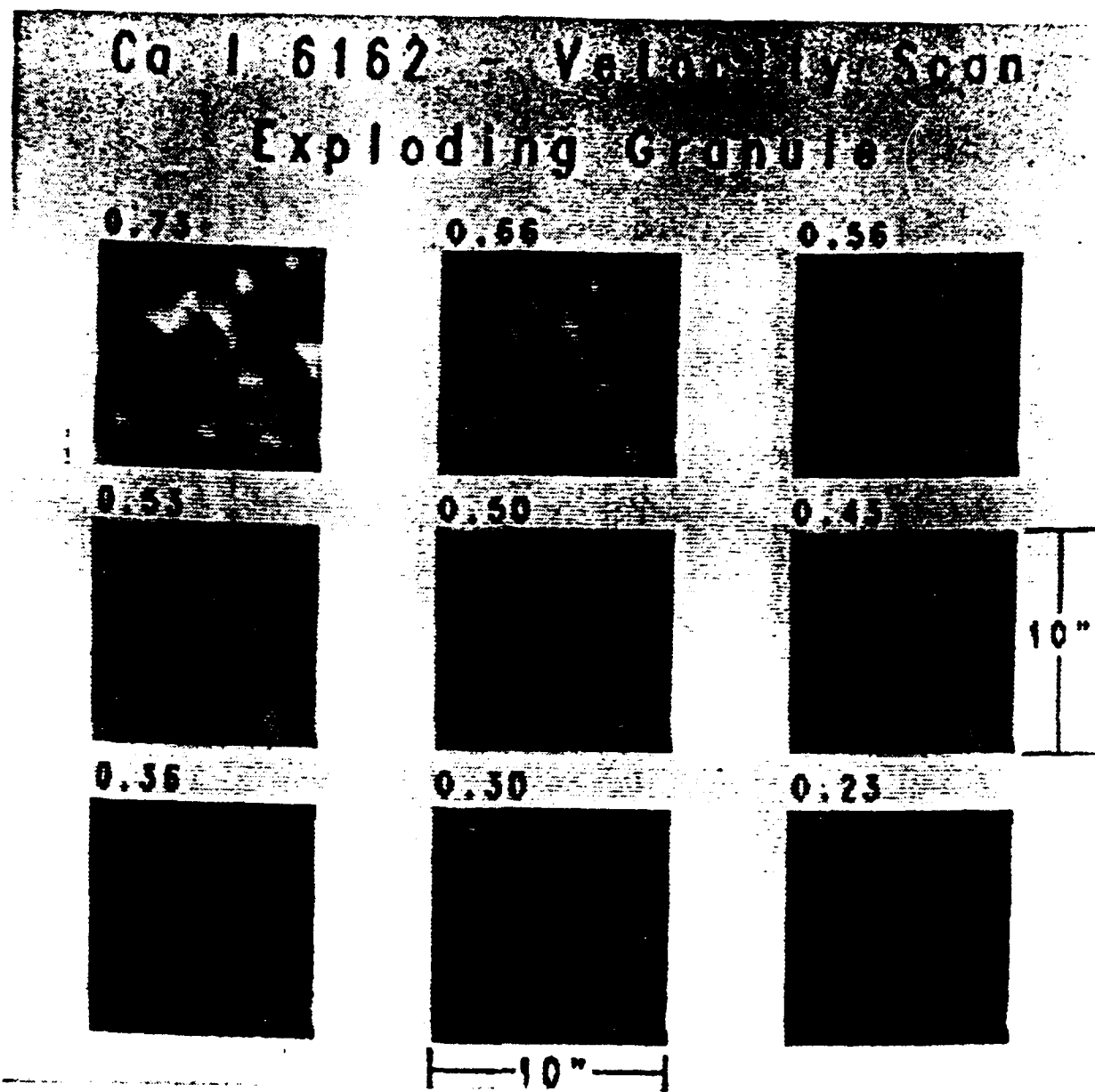


Figure 2b. This figure is similar to Figure 1b, except it shows the Dopplergrams for the expanded area around the exploding granule shown in Figure 2a. The images are again plotted from $+2.5 \text{ km s}^{-1}$ (redshifted, bright on the image) to -2.5 km s^{-1} (blueshifted, dark on the image).

cc 6152 Intensity, Soon
Exploding Granule

6161.86



6162.15



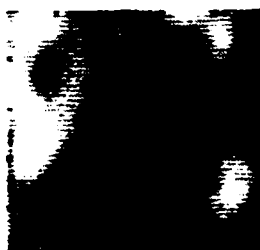
6162.31



6161.97



6162.18



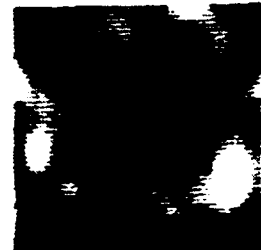
6162.39



6162.05



6162.21



6162.50



10"

Figure 2a. This figure is similar to Figure 1a, except it shows an expanded view of a region surrounding an exploding granule. The region shown is approximately $10'' \times 10''$.

Ca I 6162 - Intensity Scan

Dark Pore

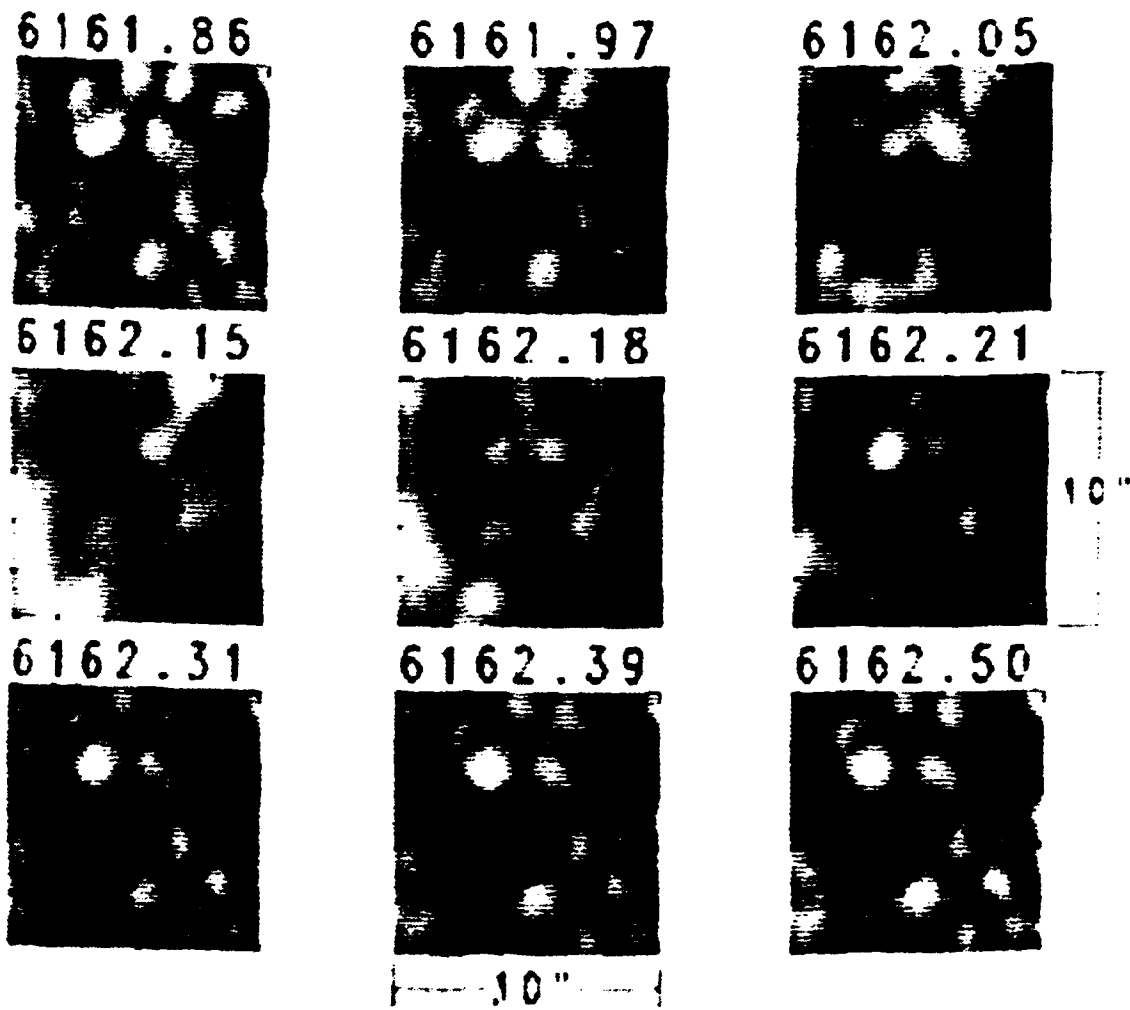


Figure 3a. This figure is similar to Figure 1a, except it shows an expanded view of a region surrounding a dark pore. The region shown is approximately $10'' \times 10''$.

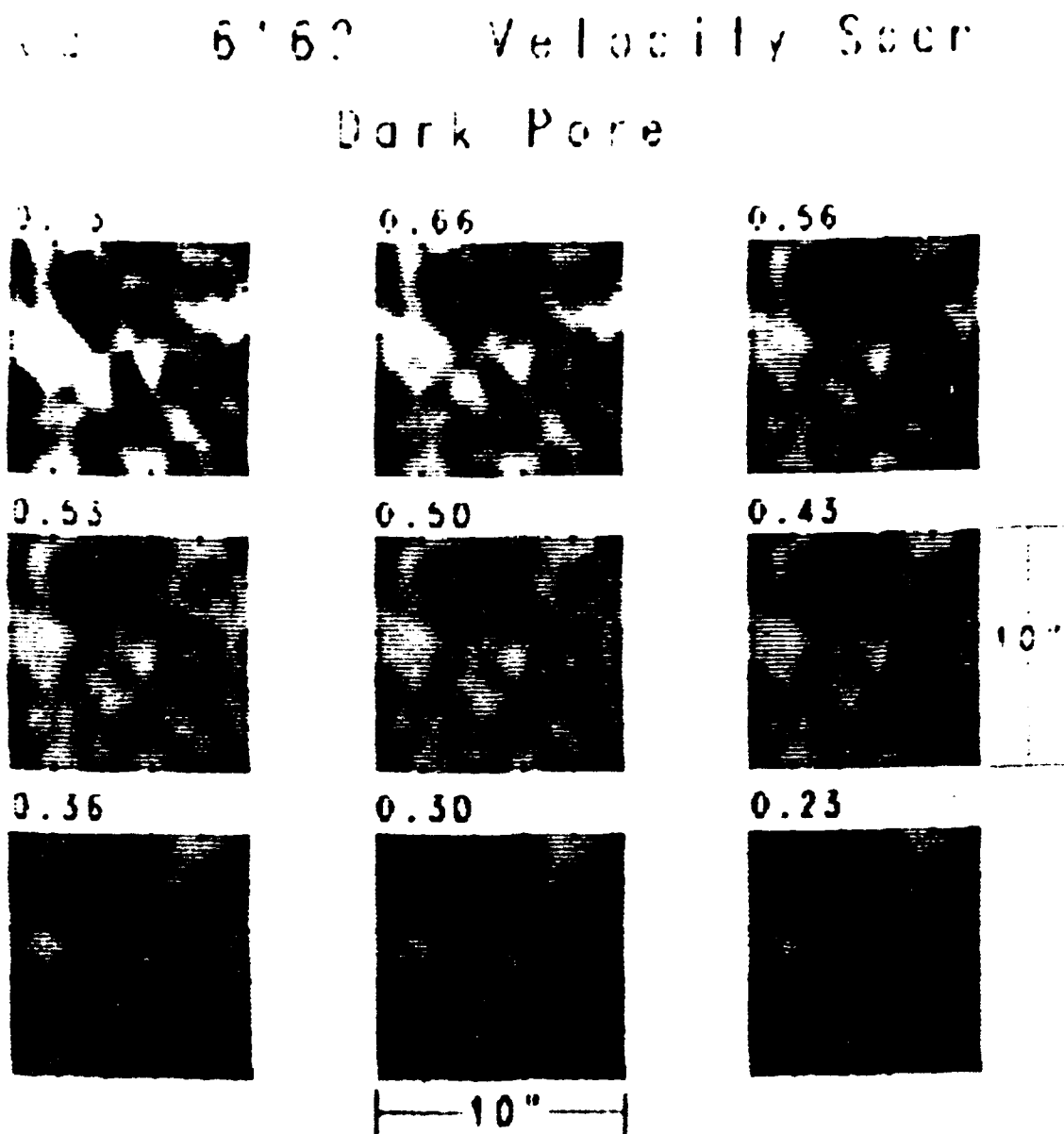


Figure 3b. This figure is similar to Figure 1b, except it shows the Dopplergrams for the expanded area around the dark pore shown in Figure 3a. The images are plotted from $+2.5 \text{ kms}^{-1}$ (redshifted, bright on the image) to -2.5 kms^{-1} (blueshifted, dark on the image).

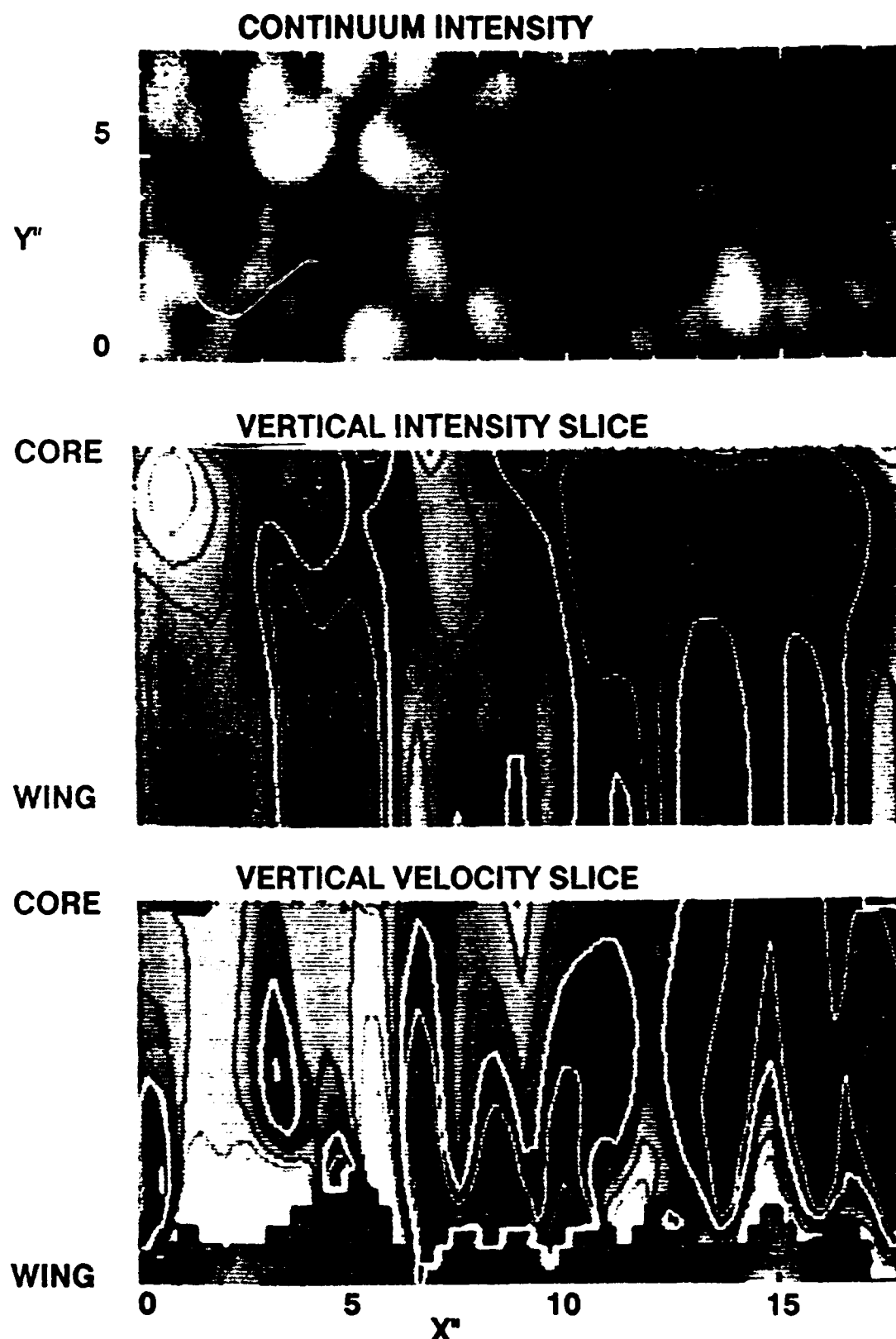


Figure 4. Intensity (middle) and vertical velocity (bottom) are shown for a vertical cross section through the data. The location of the cross section is shown on a continuum intensity map (top). The cross section passes through both the dark pore and the exploding granule. The intensity cross section is scaled from 1.16 (bright) to 0.82 (dark) times the continuum of the Jungfraujoch Atlas profile. Contours are at 0.86, 0.90, 0.94, 0.97, 1.01, 1.05, 1.09, and 1.12. The velocity cross section is scaled between 1.5 (down-flow, bright on the figure) and -1.5 km s^{-1} (dark on the figure). Contours are at -1.15, -0.83, -0.5, -0.16, 0.16, 0.5, 0.83, and 1.15 km s^{-1} .

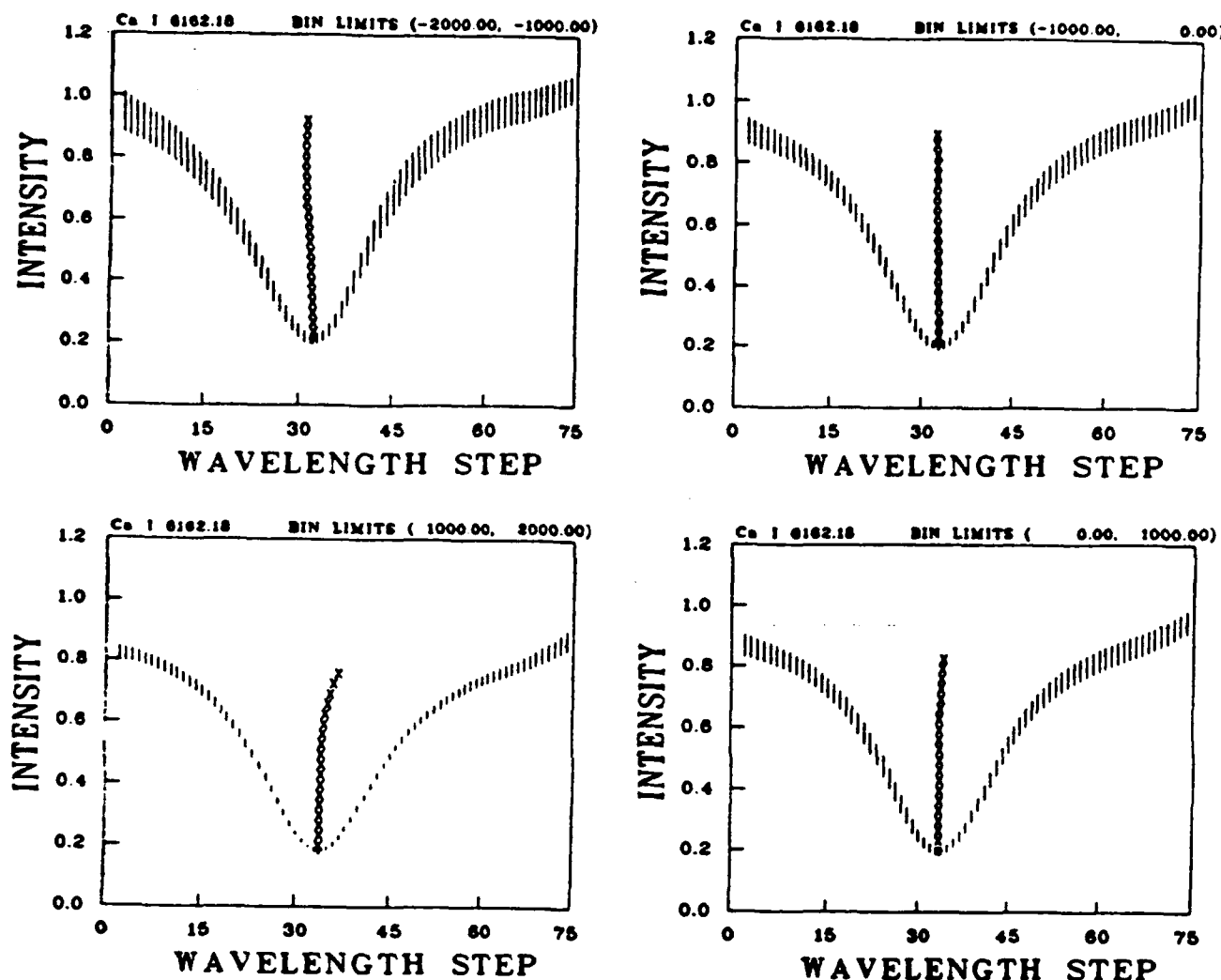


Figure 5. Average line profiles are shown for four velocity bins. Bin limits are given in ms^{-1} . One wavelength step is 10 mA. Bins are based on the velocity level observed in the line wings at the 0.75% intensity level. Negative velocity is downward (blue shifted) and positive velocity is upward (red shifted). The vertical lines represent the rms variation of the individual profiles.

The upper figures in Figure 5 show mean line profiles obtained by averaging all of the line profiles whose velocity deep in the atmosphere fell between 0 and -1000 ms^{-1} and -1000 and -2000 ms^{-1} (up-flow) and the lower figures show the result of averaging all of the profiles between 0 and $+1000 \text{ ms}^{-1}$ and $+1000$ and $+2000 \text{ ms}^{-1}$ (down-flow). The x's are the computed line bisectors at equally spaced intensity levels. The extent of the vertical lines with which the profiles are drawn, are obtained by adding and subtracting the rms variation of the individual profiles from the mean. The average profiles from up-flows have brighter wings and blueward leaning bisectors while the down-flow profiles have darker wings and redward tilted bisectors. The down-flow bisectors tend to have more curvature, perhaps caused by the fact they come from darker regions and are thus influenced more by scattered light from the bright regions. The bisectors discussed below are all obtained from similar mean profiles using different binning criteria.

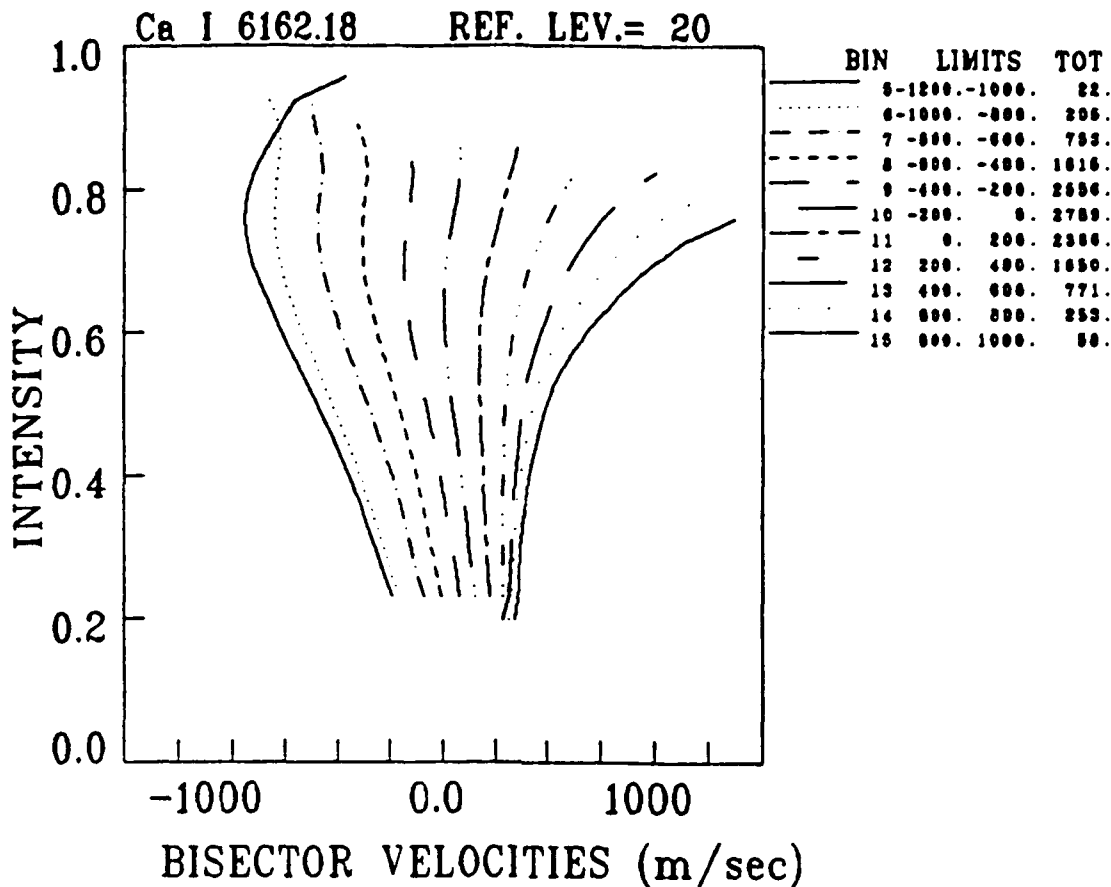


Figure 6. Bisectors of bin averaged line profiles are plotted for several bins separated by 200 ms^{-1} . Bin limits are given in ms^{-1} . The total number of profiles averaged into each bin is also shown.

In Figure 6 line bisectors measured from ensemble averages of the line profiles based on velocity bins are plotted. Average line profiles are computed by averaging together all profiles from spatial points whose velocity deep in the photosphere (as measured by the bisector shifts observed in the far wings of the line) fall into a given velocity bin. The range covered by each bin is shown in the figure. These ensemble average bisectors are much less C-shaped than bisectors obtained from spatially unresolved line profiles. The strong, blueward tilt of the up-flow bisectors can be explained by a granular flow that decreases with increasing height in the atmosphere, with a mean scale height of about 200-250 km. The down-flow bisectors are best fit with a down-flow that increases with increasing depth in the atmosphere, with a similar scale height to the up-flow, combined with about 10-20% scattered light from the up-flow regions.

Because the correlation between velocity and intensity was not 100%, bisectors from line profiles that were averaged into bins that depend on the intensity in the continuum were also computed and are shown in Figure 7. The average line profiles were computed by averaging together all profiles from spatial points whose intensity in the continuum falls into a given brightness bin. The range covered by each bin is again given in the figure. While the bisectors obtained from these ensemble average profiles are similar to those obtained by velocity averaging, they show several differences. The most striking differences are the smaller scatter of bisectors near the core and the reduced tilt of the bisectors. Many features, such as exploding granules and dark pores where several lanes intersect, have bisectors which show a wide range of shifts and tilts. Thus, mean profiles based on intensity bins include regions of both up-flow and down-flow, which probably explains most of the differences between the two sets of bisectors.

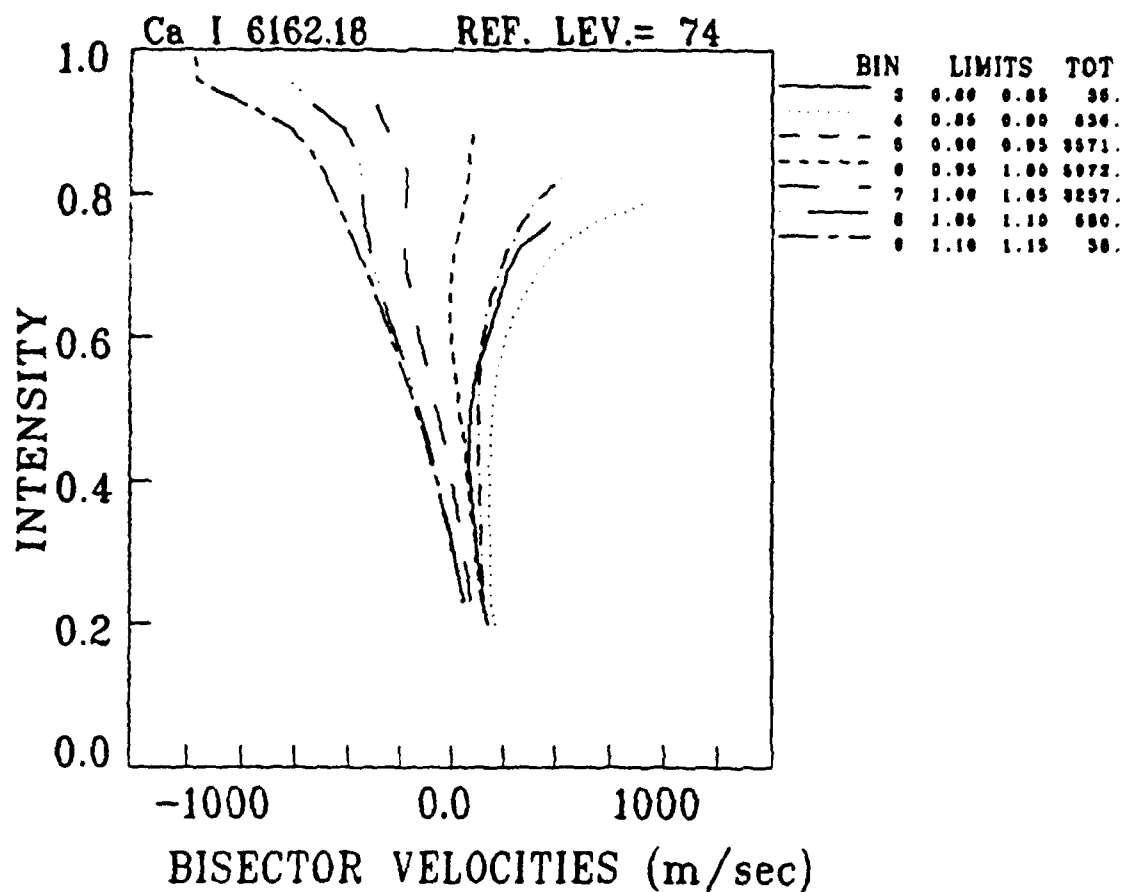


Figure 7. This figure is similar to Figure 6, only the profiles are binned based on the intensity in the continuum.

4. Discussion and Conclusions

As noted in the abstract, these data represent a very preliminary look at the observations. We plan to use the temporal variation of the filtergrams to remove the oscillations and look more carefully at the vertical flows. We also plan to observe in several more lines spanning from the deep photosphere into the chromosphere. We feel this type of narrow-band, two-dimensional spectroscopy holds great promise for understanding convective overshoot in the atmosphere.

References.

- Bonaccini, D., Smartt, R.N.: 1988, *J. Opt. Soc. Am. A* (in press)
- Bonaccini, D., Stauffer, F.: 1988, *Atron. Astrophys.* (in press)
- Canfield, R.C., Mehlretter, J.P.: 1973, *Solar Physics* 49, 3
- Dravins, D.: 1982, *Ann. Rev. Atron. Astrophys.* 20, 61
- Keil, S.L.: 1980, *Astrophys. J.* 237, 1024
- November, L.J.: 1986, *Applied Optics* 25, 392

Discussion

F. Deubner: I wonder whether you considered the possibility that the strong upward motion you observed in the center of a pore might be the instantaneous phase of a large amplitude oscillation?

P. Tamblyn: This is certainly a possibility. We have a time sequence, but have not yet analyzed it. We are currently reducing this data and will compute the temporal behavior of the motions.

S. Solanki: Could the weak correlation between downflow velocity and dark intergranular lanes which you find be due to a difference between the times at which the filtergrams used to derive the brightness and the velocity were taken?

S. Keil: The intensity map that is used to bin the profiles is from the nearby continuum and is taken about 1 sec after the line is scanned. To scan from one wing to the other takes about 1 minute. The velocity map from which the profiles were binned is from the deepest bisector level (i.e. closest to the wings of the line). Thus the velocity map is obtained from two images taken almost a minute apart. Seeing has been removed from the two images, however, part of the granulation pattern will have changed. Therefore some of the observed velocities (bisector positions) will be smeared. Partially because of this, the velocity binning and the intensity binning do not produce identical profiles. However, the velocity map from the deepest bisector levels (in the wings) correlate well with the continuum intensity image. Our bisectors are much more reliable near the line core where the temporal separation between the intensity images is smaller.